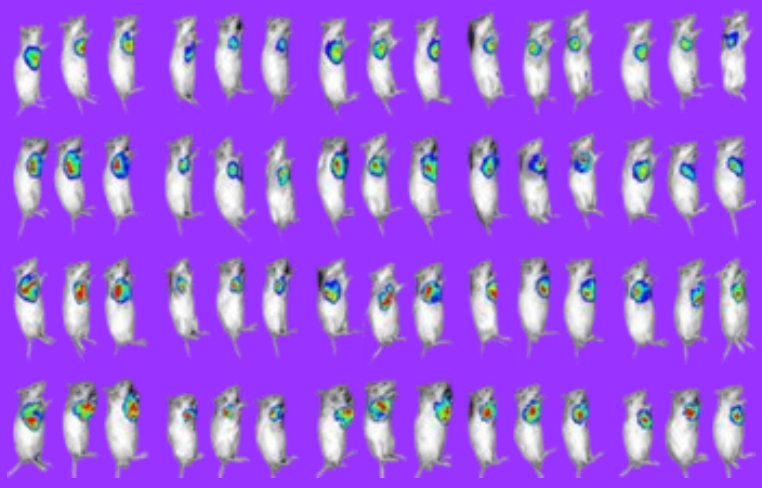

BJP

Bangladesh Journal of Pharmacology

Research Article

Cuscuta chinensis ethanol extract suppresses H22 hepatoma growth in mice and reduces PI3K/AKT phosphorylation

A Journal of the Bangladesh Pharmacological Society (BDPS)
Journal homepage: www.bdpsjournal.org; www.banglajol.info
Abstracted/indexed in Academic Search Complete, Agroforestry Abstracts, Asia Journals Online, Bangladesh Journals Online, Biological Abstracts, BIOSIS Previews, CAB Abstracts, Current Abstracts, Directory of Open Access Journals, EMBASE/Excerpta Medica, Global Health, Google Scholar, HINARI (WHO), International Pharmaceutical Abstracts, Open J-gate, Science Citation Index Expanded, SCOPUS and Social Sciences Citation Index
Bangladesh J Pharmacol 2026; 21: 108-115
ISSN: 1991-0088

Cuscuta chinensis ethanol extract suppresses H22 hepatoma growth in mice and reduces PI3K/AKT phosphorylation

Fang Tao, Yuhan Cai, Yingxiang Chen, Xiaoqiao Huang, Shuo Wang, Yang Hu, Hui Song, and Xiangming Sun

School of Pharmacy (Engineering Research Center for Medicine), Harbin University of Commerce, Harbin 150076, China.

Article Info

Received: 1 August 2026
Accepted: 5 September 2026
Available Online: 11 September 2026

DOI: 10.3329/bjp.v21i3.92463

Cite this article:
Tao F, Cai Y, Chen Y, Huang X, Wang S, Hu Y, Song H, Sun X. *Cuscuta chinensis* ethanol extract suppresses H22 hepatoma growth in mice and reduces PI3K/AKT phosphorylation. Bangladesh J Pharmacol. 2026; 21: 108-115.

Abstract

This study evaluated the effects of *Cuscuta chinensis* ethanol extract in H22 hepatoma-bearing mice. Tumor-bearing mice were treated with cyclophosphamide or varying doses of the extract for 14 days. Tumor growth was assessed using bioluminescence imaging and tumor weight measurements. The extract slowed the increase in bioluminescence and reduced tumor weight, achieving a maximum inhibition rate of 50.4%. It decreased the spleen index, increased the thymus index at the two higher doses, elevated serum interleukin-2 levels at the two higher doses, and increased tumor necrosis factor-α at all doses. Additionally, it reduced alpha-fetoprotein levels at the two higher doses. Histological analysis of tumor tissue revealed degenerative and necrotic changes. The extract increased Bax expression and the Bax/Bcl-2 ratio at all doses while reducing Bcl-2 expression at the two higher doses. Total PI3K and AKT levels remained largely unchanged; however, their phosphorylated forms and phosphorylation ratios were reduced. Overall, the extract inhibited H22 tumor growth, accompanied by modulation of apoptosis-related proteins and decreased phosphorylation of PI3K and AKT.

Introduction

Primary liver cancer is most commonly represented by hepatocellular carcinoma, which remains a leading cause of global cancer mortality (Bray et al., 2024). Although patients diagnosed at an early stage may benefit from curative treatments such as resection, local ablation, or liver transplantation, many present with advanced disease stages when these options are no longer viable (Llovet et al., 2021; Reig et al., 2022; Singal et al., 2023). While systemic therapies have advanced with targeted drugs and immunotherapy combinations, intrinsic and acquired resistance often limit long-term outcomes (Yang et al., 2024; Zheng et al., 2025). In this context, naturally derived substances remain a vital source of chemically diverse compounds for the development of novel antineoplastic agents (Newman and Cragg, 2020; Yu et al., 2020; Gao et al., 2024).

Cuscuta chinensis Lam. (Convolvulaceae) is used in traditional Chinese medicine primarily to tonify the liver and kidneys and to treat reproductive and urinary disorders. Flavonoids, phenolic acids, lignans, organic acids, and terpenoids have been identified in this species (Donnapee et al., 2014; Sun et al., 2025). Preparations of *C. chinensis* have demonstrated growth-inhibitory effects in cancer cells (Dermani et al., 2021), and an extract from the related species *C. reflexa* reduced tumor burden in a murine colon cancer model (Mishra et al., 2022). Previous studies showed that a

95% ethanol extract of *C. chinensis* reduced HepG2 cell viability and modulated PI3K/AKT-related proteins in breast cancer models; however, its effect on hepatoma growth *in vivo* has not yet been evaluated (Song et al., 2024; Song et al., 2025; Tang, 2023).

The PI3K/AKT pathway regulates cell survival, proliferation, and metabolism and is frequently dysregulated in hepatocellular carcinoma (Hoxhaj and Manning, 2020; Manning and Toker, 2017; Zheng et al., 2025). Bax and Bcl-2 are involved in regulating mitochondrial apoptotic signaling (Elmore, 2007). Therefore, the present study evaluated the effects of *C. chinensis* ethanol extract in H22 hepatoma-bearing mice using serial bioluminescence imaging, endpoint tumor weight measurement, and histological analysis. Serum markers, as well as thymus and spleen indices, were also assessed. Total and phosphorylated PI3K and AKT levels were measured to assess pathway phosphorylation, while Bax and Bcl-2 expression was examined to determine whether tumor inhibition was accompanied by changes in the balance of apoptosis-related proteins.

Materials and Methods

Plant collection and extraction procedure

The dried, ripe seeds of *C. chinensis* were sourced from a cultivation site in Luobei County, Heilongjiang Province, China. Botanical identification was performed by Prof. Zhongyuan Qu of the School of Pharmacy, Harbin University of Commerce, where a reference specimen (HM2020102402) has been preserved. After being ground into powder, the seeds underwent overnight maceration with 95% ethanol at a 1:10 (w/v) solid-to-liquid ratio. Reflux extraction was subsequently performed for 1 hour, repeated for three consecutive cycles.

Cell line and reagents

Luciferase-expressing murine H22 hepatoma cells and the LUC1 luciferase substrate were sourced from Zhejiang Meisen Cell Technology Co., Ltd. (China). Cyclophosphamide tablets were purchased from Tonghua Maoxiang Pharmaceutical Co., Ltd. (China). ELISA kits for measuring mouse interleukin-2 (IL-2), tumor necrosis factor-α (TNF-α), and alpha-fetoprotein were obtained from Shanghai Enzyme-linked Biotechnology Co., Ltd. (China). Primary antibodies targeting PI3K, p-PI3K, AKT, p-AKT, Bax, and Bcl-2 were procured from Wanleibio Co., Ltd. (China), while the anti-β-actin primary antibody was sourced from Bioss Antibodies (China). Beyotime Biotechnology (China) supplied the horseradish peroxidase-conjugated goat anti-rabbit secondary antibody and RIPA lysis buffer. Phenylmethylsulfonyl fluoride and enhanced chemiluminescence reagent were purchased from Meilun Biotechnology (China), and nitrocellulose membranes were produced by Pall China Co., Ltd. (China).

Animals

Male Kunming mice (weighing 18 ± 2 g) were provided by the Laboratory Animal Center of Harbin Medical University under permit number SYXK [Hei] 2019-001. The mice were housed in a barrier environment maintained at 22–25°C with 40–70% relative humidity, with unrestricted access to food and water. After a 7-day environmental adaptation period, all experimental protocols commenced.

H22 tumor model, grouping and treatment

Luciferase-tagged H22 cells were initially expanded via the intraperitoneal route in donor mice. For inoculation, cell pellets were resuspended in PBS to a final concentration of 1×10^7 cells/mL, followed by intraperi-toneal administration of 200 µL per animal. Approximately 7 days later, ascitic fluid was collected. The cells were isolated by centrifugation, resuspended in normal saline, and adjusted to 1×10^7 cells/mL. For tumor induction, each mouse received 200 µL of the cell suspension, corresponding to 2×10^6 cells, by subcutaneous injection into the right axillary region.

When palpable tumors developed, the tumor-bearing mice were randomly assigned to the model group, the cyclophosphamide group, or groups receiving different doses of the extract. Eight non-inoculated mice served as the non-tumor control group. Each group consisted of eight mice. The extract was suspended in normal saline and administered once daily by oral gavage at doses of 3.1, 6.2, or 12.4 g/kg/day. Cyclophosphamide was administered intragastrically at a dose of 20 mg/kg. Mice in both the normal control and model groups received an equivalent volume of physiological saline. The treatment period lasted for 14 consecutive days.

Assessment of tumor growth and organ indices

Body weight was recorded throughout the treatment period. Before the first imaging session, three mice were randomly selected from each tumor-bearing group, and the same animals were imaged on treatment days 5, 8, 11, and 14. Ten minutes before imaging, the mice received an intraperitoneal injection of LUC1 luciferase substrate solution at a dose of 150 mg/kg (15 mg/mL; 10 µL/g). The mice were anesthetized with isoflurane, and images were acquired using a PE IVIS Lumina III small-animal imaging system (PerkinElmer, USA) with consistent acquisition settings at each time point. A region of interest was drawn over the tumor, and photon flux was quantified using the instrument software and expressed as photons per second.

Following the final dose, mice were humanely euthanized to collect tumor, thymus, and spleen tissues from each individual for weight measurement. Tumor

growth inhibition was assessed using the tumor inhibition percentage (%):

Tumor inhibition rate (%) = [(mean tumor weight of the model group − mean tumor weight of the treatment group) ÷ mean tumor weight of the model group] × 100

The thymus and spleen indices were calculated as the organ weight (mg) divided by the final body weight (g). Endpoint tumor and organ weights were measured in all eight mice per group.

Serum assays and histopathology

Whole blood was incubated at room temperature for 30 min followed by storage at 4°C. Serum was isolated by centrifugation at 4,000 rpm for 15 minutes. Serum levels of IL-2, TNF-α, and alpha-fetoprotein were quantified using commercial ELISA kits according to the suppliers' protocols. Serum samples from six mice per group were analyzed. Tumor tissue was fixed in 10% neutral buffered formalin, processed through an ascending ethanol series, embedded in paraffin, and sectioned at a thickness of 3 µm. The sections were then deparaffinized, rehydrated, and stained with hematoxylin and eosin. Morphological changes were evaluated descriptively using a light microscope.

Western blotting

Tumor tissues were homogenized in RIPA lysis buffer supplemented with phenylmethylsulfonyl fluoride and kept on ice for cell lysis. The homogenates were centrifuged at 12,000 rpm for 10 min, after which protein concentrations in the resulting supernatant were quantified using the Bradford method (Jankovskaja et al., 2019). Equal amounts of total protein were separated by SDS-PAGE and electroblotted onto nitrocellulose membranes. After blocking with 5% non-fat milk for 2 hours at room temperature, the membranes were incubated overnight at 4°C with primary antibodies against PI3K, p-PI3K, AKT, p-AKT, Bax, Bcl-2, or β-actin, each diluted 1:500. Following washing steps, the membranes were incubated with an HRP-conjugated secondary antibody (1:1,000) for 1 hour at room temperature. Specific protein bands were visualized using enhanced chemiluminescence reagents and quantified with Image Lab software. Signal intensity for each target protein was normalized to β-actin from the corresponding lane on the same membrane. Phosphorylation levels of PI3K and AKT were calculated as the ratio of normalized p-PI3K to total PI3K and normalized p-AKT to total AKT, respectively. The Bax/Bcl-2 ratio was determined from the normalized signal intensities of Bax and Bcl-2. Tumor tissues from three different mice in each group were analyzed.

Statistical analysis

Data are expressed as the mean ± standard deviation. Group comparisons were evaluated using one-way ANOVA, followed by Tukey's post hoc test for multiple comparisons. Body weight and bioluminescence data were analyzed separately at each time point. All statistical calculations were performed using SPSS Statistics 26.0, while visualizations were generated with GraphPad Prism 9.5.0. Statistical significance was set at $p<0.05$.

Results

Percentage yield of extract

The ethanol extract of *C. chinensis* was obtained with a yield of 14.8% relative to the initial dry weight of the seeds.

Extract suppresses tumor growth in H22 hepatoma-bearing mice

Body weights were similar among the tumor-bearing groups on treatment days 5, 8, and 11. On day 14, body weight was significantly higher in the high-dose extract group and significantly lower in the cyclophosphamide group compared to the model group ($p<0.05$; Figure 1A).

Bioluminescence increased over time in all tumor-bearing groups. No differences among the groups were observed on day 5 or 8. On day 11, the signal was significantly lower than the model value in the low-dose extract group ($p<0.05$) and in the medium- and high-dose groups ($p<0.01$). All three extract groups exhibited lower signals than the model group on day 14 ($p<0.01$; Figure 1B and C). The cyclophosphamide group also showed significantly lower signals on day 11 and 14 ($p<0.01$).

At the conclusion of treatment, tumor weight in the model group was significantly higher compared to the non-tumor control group. Administration of the extract at all three doses resulted in a significant reduction in tumor weight compared to the model group ($p<0.01$), with inhibition rates of 23.8%, 39.3%, and 50.4% for the low, medium, and high doses, respectively (Figure 1D and E). These findings were consistent with the bioluminescence imaging data and demonstrated a dose-dependent antitumor effect. Cyclophosphamide also significantly reduced tumor weight ($p<0.01$).

Compared to the non-tumor control group, the model group exhibited an increased spleen index and a decreased thymus index ($p<0.01$; Figure 1F and G). Treatment with the extract at all three doses significantly reduced the spleen index ($p<0.01$). The medium and high doses of the extract significantly increased the thymus index ($p<0.01$), while the low dose did not produce a significant change. Cyclophosphamide treatment also significantly decreased the spleen index ($p<0.01$) but did not significantly affect the thymus index compared to the model group.

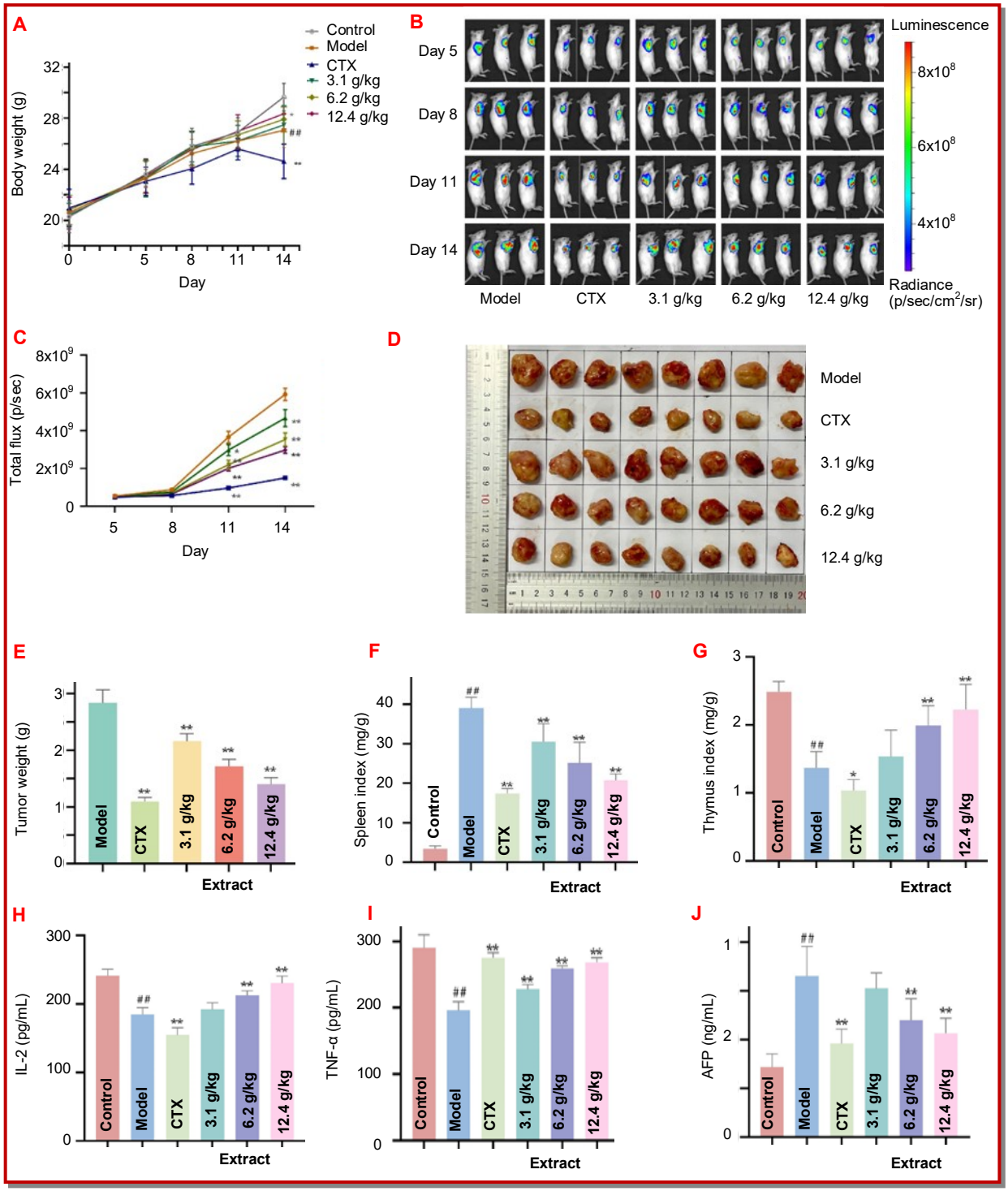

Figure 1. Effects of *C. chinensis* ethanol extract on different parameters in H22 hepatoma-bearing mice. Body weight during 14 days of treatment (A); representative bioluminescence images on days 5, 8, 11, and 14 (B); tumor-associated bioluminescence (C); excised tumors (D); endpoint tumor weight (E); spleen index (F); thymus index (G), interleukin-2 (IL-2)(H); tumor necrosis factor-α (TNF-α)(I); and alpha-fetoprotein (AFP) (J). Values are mean ± SD. n=8; bioluminescence imaging: n=3. ##p<0.01 versus the non-tumor control group; *p<0.05 and **p<0.01 versus the model group. CTX means cyclophosphamide

Extract alters serum indices and tumor morphology

Compared to the non-tumor control group, the model group exhibited lower serum levels of IL-2 and TNF-α, along with a higher alpha-fetoprotein level (p<0.01; Figure 1H–J). Relative to the model group, medium- and high-dose extract treatments increased IL-2 levels,

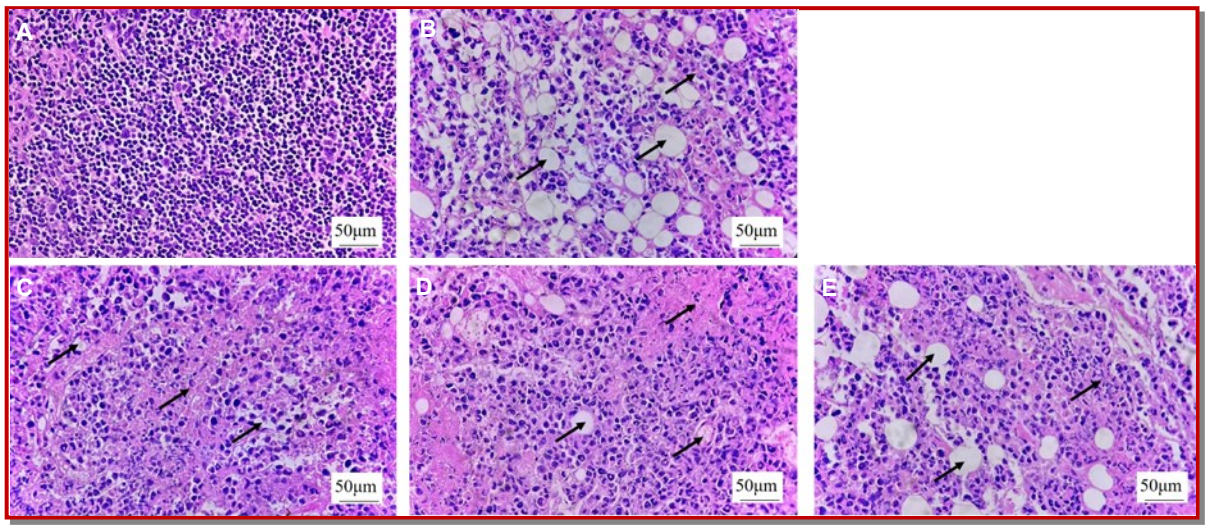

Figure 2. Effects of *C. chinensis* ethanol extract on tumor histology in H22 hepatoma-bearing mice. Representative hematoxylin and eosin-stained tumor sections after 14 days of treatment. Arrows indicate areas with loss of cellular integrity, nuclear dissolution or necrotic change. the groups are: Model (A), cyclophosphamide (B), extract doses 3.1 g/kg (C), 6.2 g/kg (D), and 12.4 g/kg (E). Scale bar=50 μm

while all three doses elevated TNF-α levels ($p<0.01$). Additionally, moderate- and high-dose treatments suppressed alpha-fetoprotein secretion ($p<0.01$). The low dose did not significantly affect IL-2 or alpha-fetoprotein levels. Cyclophosphamide administration resulted in decreased IL-2 and alpha-fetoprotein levels but caused an increase in TNF-α compared to the model group ($p<0.01$).

Neoplastic cells in the model group maintained structural integrity, exhibiting well-defined cellular boundaries along with enlarged, hyperchromatic nuclei. Tumors treated with the extract showed loss of cell integrity, paler staining, nuclear dissolution, and necrotic areas. These changes were most pronounced at the high dose. Cyclophosphamide produced similar and more pronounced histological changes (Figure 2).

Extract alters PI3K/AKT phosphorylation and Bax/Bcl-2 expression in tumor tissue

Representative immunoblots and expression levels are shown in Figure 3. Total PI3K and AKT expression did not vary significantly across the model and treated cohorts. All three extract doses reduced p-PI3K levels and the p-PI3K/PI3K ratio ($p<0.01$), accompanied by corresponding decreases in p-AKT expression and the p-AKT/AKT ratio ($p<0.01$). Cyclophosphamide produced similar reductions ($p<0.01$).

Relative to the model group, Bax levels were elevated across all three extract groups ($p<0.05$ for the low dose; $p<0.01$ for the moderate and high doses). Bcl-2 expression was downregulated in the medium- and high-dose groups ($p<0.01$), but did not differ significantly at the low dose. The Bax/Bcl-2 ratio was higher in all three extract groups ($p<0.05$ at the low dose; $p<0.01$ at the moderate and high doses). Cyclophosphamide similarly augmented Bax levels and the Bax/Bcl-2 ratio while suppressing Bcl-2 expression ($p<0.01$).

Discussion

Hyperoside is a flavonoid compound and serves as a quality control marker for *C. chinensis* in the Chinese Pharmacopoeia (Chinese Pharmacopoeia Commission, 2025). On a crude drug weight basis, its content in the ethanol extract was 2.8 ± 0.1 mg/g (Sun et al., 2020).

The extract suppressed H22 tumor growth in mice. Serial bioluminescence imaging revealed that differences from the model group emerged during the later treatment period, and the endpoint tumor weights supported this pattern. The high-dose group exhibited the greatest inhibition. Thus, both dynamic imaging and endpoint measurements demonstrated a reduction in tumor burden. Growth-inhibitory effects of other plant extracts have also been reported in tumor-bearing mice (He et al., 2016; Ramalingam and Renuka, 2025).

Histological examination revealed loss of cellular integrity, pale staining, nuclear dissolution, and necrotic areas in extract-treated tumors. These changes were most pronounced in the high-dose group. Similar degenerative and necrotic alterations have been reported in other H22 studies where tumor growth was inhibited (Xu et al., 2018; Lu et al., 2023). Bax and Bcl-2 regulate mitochondrial apoptotic signaling (Elmore, 2007). The extract increased Bax expression and the Bax/Bcl-2 ratio at all three doses, while Bcl-2 expression decreased at the medium and high doses. This pattern indicates a shift in the balance of apoptosis-related proteins toward a pro-apoptotic state. However, apoptosis was not directly measured, so these protein chan-

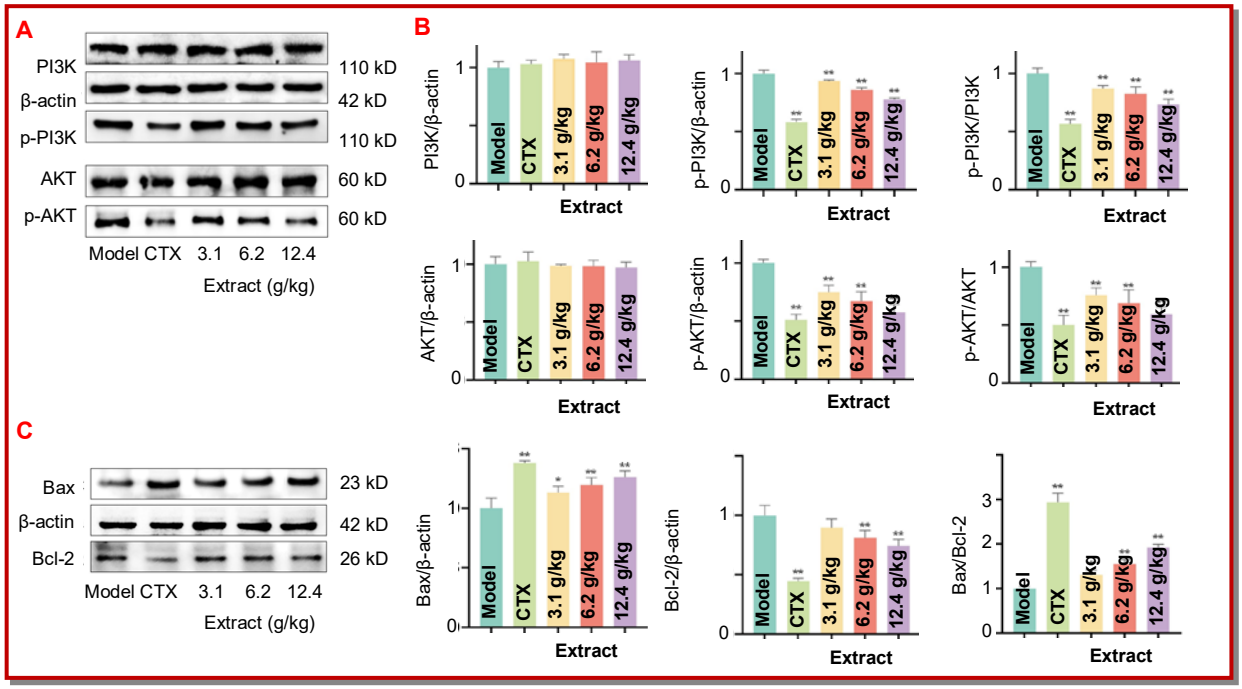

Figure 3. Effects of *C. chinensis* ethanol extract on protein expression in tumor tissues (A), different parameters (B), and expression (C) in H22 hepatoma-bearing mice. (A) Representative immunoblots of PI3K, p-PI3K, AKT, p-AKT, and their corresponding β-actin loading controls. Data are presented as mean ± SD (n=3 mice per group). **p<0.01 versus the model group. CTX, cyclophosphamide

ges should not be considered definitive evidence that apoptosis caused the reduction in tumor growth.

Tumor progression is influenced by both malignant cells and the host immune environment (Donne and Lujambio, 2023). The extract also altered splenic and thymic indices, as well as serum levels of IL-2, TNF-α, and alpha-fetoprotein. All three doses reduced the spleen index, whereas medium and high doses elevated the thymus index. Serum IL-2 was upregulated in response to the medium and high doses; TNF-α increased across all three dose groups, and alpha-fetoprotein declined at the medium and high doses. Organ indices and circulating cytokines have also been used to describe tumor- and treatment-related changes in H22 models (Ling et al., 2017; Liu et al., 2021; Qiao et al., 2020). These changes may reflect the host response to tumor growth and treatment, although analysis of immune cell subsets is necessary to define their immunological significance.

PI3K/AKT signaling regulates cell survival, proliferation, and metabolism and is frequently altered in hepatocellular carcinoma (Hoxhaj and Manning, 2020; Manning and Toker, 2017; Zheng et al., 2025). The extract did not significantly alter total PI3K or AKT levels. In contrast, phosphorylated PI3K (p-PI3K) and phosphorylated AKT (p-AKT) levels, as well as their ratios to the corresponding total proteins, were reduced. This pattern indicates decreased phosphorylation of PI3K and AKT rather than a reduction in the total protein abundance. The phosphorylation changes occurred alongside a reduction in tumor burden. Because no pathway-specific inhibitor, activator, or genetic intervention was used, whether reduced PI3K/AKT phosphorylation directly contributed to tumor inhibition remains unresolved.

Conclusion

The extract suppressed H22 tumor growth in mice, and tumor inhibition was accompanied by changes in tumor morphology, spleen and thymus indices, serum IL-2, TNF-α, and alpha-fetoprotein levels, a higher Bax/Bcl-2 ratio, and reduced PI3K and AKT phosphorylation. These findings provide *in vivo* evidence for the extract's antitumor activity, although the causal role of PI3K/AKT signaling remains to be established.

Financial Support

This work was supported by the Natural Science Foundation of Heilongjiang Province (LH2024H036) and the Heilongjiang Province "Double First-Class" Discipline Collaborative Innovation Achievement Project (LJGXCG2024-P33)

Ethical Issue

The Experimental Animal Ethics Committee of Harbin University of Commerce approved the animal procedures (No. HSDYXY-2024061). Following a 7-day environmental

adaptation period, all experimental protocols received formal authorization from the Committee. Every animal procedure strictly adhered to established guidelines governing laboratory animal welfare and care

Conflict of Interest

Authors declare no conflict of interest

References

Bray F, Laversanne M, Sung H, Ferlay J, Siegel RL, Soerjomataram I, Jemal A. Global cancer statistics 2022: GLOBOCAN estimates of incidence and mortality worldwide for 36 cancers in 185 countries. CA Cancer J Clin. 2024; 74: 229-63.

Chinese Pharmacopoeia Commission. Pharmacopoeia of the People's Republic of China: Volume I. 2025 ed. Beijing, China Medical Science Press, 2025.

Dermani FK, Saidijam M, Najafi R, Moradkhani S, Mohammadzaheri Z, Beiranvand N, Mohammadi S, Shabab N, Kalvandi R, Zeraati F. Cytotoxic effects of hydroalcoholic extract of *Cuscuta chinensis* on PC3 and MCF7 cancer cell lines. Avicenna J Phytomed. 2021; 11: 258.

Donne R, Lujambio A. The liver cancer immune micro-environment: Therapeutic implications for hepatocellular carcinoma. Hepatology 2023; 77: 1773-96.

Donnapee S, Li J, Yang X, Ge AH, Donkor PO, Gao XM, Chang YX. *Cuscuta chinensis* Lam.: A systematic review on ethnopharmacology, phytochemistry and pharmacology of an important traditional herbal medicine. J Ethnopharmacol. 2014; 157: 292-308.

Elmore S. Apoptosis: A review of programmed cell death. Toxicol Pathol. 2007; 35: 495-516.

Gao S, Tan H, Gang J. Inhibition of hepatocellular carcinoma cell proliferation through regulation of the cell cycle, AGE-RAGE, and leptin signaling pathways by a compound formulation comprised of andrographolide, wogonin, and oroxylin A derived from *Andrographis paniculata* (Burm.f.) Nees. J Ethnopharmacol. 2024; 329: 118001.

He Z, Jiang C, Zhang J, Yin ZQ, Yin ZF, Zhu Y, Fu J. Neem tree (*Azadirachta indica*) extract specifically suppresses the growth of tumors in H22-bearing Kunming mice. Z Naturforsch C J Biosci. 2016; 71: 201-08.

Hoxhaj G, Manning BD. The PI3K-AKT network at the interface of oncogenic signalling and cancer metabolism. Nat Rev Cancer. 2020; 20: 74-88.

Jankovskaja S, Kamiie J, Rezeli M, Gustavsson L, Sugihara Y, Miliotis T, Ruzgas T, Marko-Varga G. Optimization of sample preparation for transporter protein quantification in tissues by LC–MS/MS. J Pharm Biomed Anal. 2019; 164: 9-15.

Ling N, Zhou X, Ji Y, Li W, Ji C, Qi Z. Immuno-modulatory and cellular antioxidant activities of κ-selenocarrageenan in combination with epirubicin in H22 hepatoma-bearing mice. Biomed Pharmacother. 2017; 91: 132-37.

Liu YH, Qin HY, Zhong YY, Li S, Wang HJ, Wang H, Chen LL, Tang X, Li YL, Qian ZY, Li HY, Zhang L, Chen T. Neutral polysaccharide from *Panax notoginseng* enhanced cyclophosphamide antitumor efficacy in hepatoma H22-bearing mice. BMC Cancer. 2021; 21: 37.

Llovet JM, Kelley RK, Villanueva A, Singal AG, Pikarsky E, Roayaie S, Lencioni R, Koike K, Zucman-Rossi J, Finn RS. Hepatocellular carcinoma. Nat Rev Dis Primers. 2021; 7: 6.

Lu Y, Zhang S, Zhu X, Wang K, He Y, Liu C, Sun J, Pan J, Zheng L, Liu W, Li Y, Huang Y, Liu T. Aidi injection enhances the anti-tumor impact of doxorubicin in H22 tumor-containing mice. J Ethnopharmacol. 2023; 303: 115968.

Manning BD, Toker A. AKT/PKB signaling: Navigating the network. Cell 2017; 169: 381-405.

Mishra S, Alhodieb FS, Barkat MA, Hassan MZ, Barkat HA, Ali R, Alam P, Alam O. Antitumor and hepatoprotective effect of *Cuscuta reflexa* Roxb. in a murine model of colon cancer. J Ethnopharmacol. 2022; 282: 114597.

Newman DJ, Cragg GM. Natural products as sources of new drugs over the nearly four decades from 1981 to 2019. J Nat Prod. 2020; 83: 770-803.

Qiao Y, Cao Y, Yu K, Zong L, Pu X. Preparation and antitumor evaluation of quercetin nanosuspensions with synergistic efficacy and regulating immunity. Int J Pharm. 2020; 589: 119830.

Ramalingam S, Renuka S. Anti-tumor activity of *Simarouba glauca* on Ehrlich ascites carcinoma in mice. Bangladesh J Pharmacol. 2025; 20: 113-21.

Reig M, Forner A, Rimola J, Ferrer-Fabrega J, Burrel M, Garcia-Criado A, Kelley RK, Galle PR, Mazzaferro V, Salem R, Sangro B, Singal AG, Vogel A, Fuster J, Ayuso C, Bruix J. BCLC strategy for prognosis prediction and treatment recommendation: The 2022 update. J Hepatol. 2022; 76: 681-93.

Singal AG, Llovet JM, Yarchoan M, Mehta N, Heimbach JK, Dawson LA, Jou JH, Kulik LM, Agopian VG, Marrero JA, Mendiratta-Lala M, Brown DB, Rilling WS, Goyal L, Wei AC, Taddei TH. AASLD practice guidance on prevention, diagnosis, and treatment of hepatocellular carcinoma. Hepatology 2023; 78: 1922-65.

Song H, Huang XQ, Sun XM, Tang J, Wang YH, Han XN, Li WL. Mechanism of alcohol extract of *Cuscuta chinensis* against breast cancer based on network pharmacology, molecular docking and animal experiments. Chin Tradit Herb Drugs. 2024; 55: 4747-58. [in Chinese]

Song H, Wang YH, Huang XQ, Sun XM, Lang L, Shan WC, Tang J, Yu L, Ji CF. Screening of active fractions of *Cuscuta chinensis* and investigation of its anti-breast cancer mechanism. J Hainan Med Univ. 2025; 31: 1869-77. [in Chinese]

Sun XM, Song H, Yan XJ, Hu Y, Xu BL, Zhao LZ, Li WL. Screening and determination of estrogen-like quality markers of *Cuscuta chinensis*. Chin Tradit Herb Drugs. 2020; 51: 2671-79.

Sun X, Zhao M, Liang W, Song H, Qu Z, Sui L, Li W. Reverse traceability analysis of estrogenic active ingredients in Cuscutae Semen based on intestinal and hepatic metabolism. J Pharm Biomed Anal. 2025; 260: 116819.

Tang J. Study on the mechanism of *Cuscuta chinensis* against

breast cancer based on the PI3K/AKT signaling pathway. M.Sc. Thesis, Harbin University of Commerce, 2023. [in Chinese]

Xu Q, Gu J, Lv Y, Yuan J, Yang N, Chen J, Wang C, Hou X, Jia X, Feng L, Yin G. Angiogenesis for tumor vascular normalization of endostar on hepatoma 22 tumor-bearing mice is involved in the immune response. Oncol Lett. 2018; 15: 3437-46.

Yang X, Yang C, Zhang S, Geng H, Zhu AX, Bernards R, Qin W, Fan J, Wang C, Gao Q. Precision treatment in advanced hepatocellular carcinoma. Cancer Cell. 2024; 42: 180-97.

Yu L, Shang D, Lang L, Liu Y, Yu M, Song D, Jia S, Han S, Li C, Liu J, Xu Y, Zhang X. TMF, a natural dihydroflavonoid isolated from *Scutellaria javanica* Jungh, stimulates anticancer activity of S180 cancer-bearing mice, induces apoptosis, and inhibits invasion and migration of HepG2 cells. J Ethnopharmacol. 2020; 263: 113072.

Zheng J, Wang S, Xia L, Sun Z, Chan KM, Bernards R, Qin W, Chen J, Xia Q, Jin H. Hepatocellular carcinoma: Signaling pathways and therapeutic advances. Signal Transduct Target Ther. 2025; 10: 35.

Author Info

Hui Song and Xiangming Sun (Principal contact)
e-mail: huihui4595@sina.com; sunxiangming2002@163.com